

REPORT DOCUMENTATION PAGE

Form Approved
OMB No. 0704-0188

The public reporting burden for this collection of information is estimated to average 1 hour per response, including the time for reviewing instructions, searching existing data sources, gathering and maintaining the data needed, and completing and reviewing the collection of information. Send comments regarding this burden estimate or any other aspect of this collection of information, including suggestions for reducing the burden, to Department of Defense, Washington Headquarters Services, Directorate for Information Operations and Reports (0704-0188), 1215 Jefferson Davis Highway, Suite 1204, Arlington, VA 22202-4302. Respondents should be aware that notwithstanding any other provision of law, no person shall be subject to any penalty for failing to comply with a collection of information if it does not display a currently valid OMB control number.
PLEASE DO NOT RETURN YOUR FORM TO THE ABOVE ADDRESS.

1. REPORT DATE (DD-MM-YYYY) 08/29/2014		2. REPORT TYPE Final Technical		3. DATES COVERED (From - To) 6/2010 to 9/2014	
4. TITLE AND SUBTITLE Chaotic Lidar for Naval Applications				5a. CONTRACT NUMBER	
				5b. GRANT NUMBER N00014-10-1-0906	
				5c. PROGRAM ELEMENT NUMBER	
6. AUTHOR(S) William D. Jemison				5d. PROJECT NUMBER	
				5e. TASK NUMBER 1	
				5f. WORK UNIT NUMBER	
7. PERFORMING ORGANIZATION NAME(S) AND ADDRESS(ES) Clarkson University Office Of Grants And Contracts Potsdam, NY 13699-5605				8. PERFORMING ORGANIZATION REPORT NUMBER	
9. SPONSORING/MONITORING AGENCY NAME(S) AND ADDRESS(ES) Office of Naval Research 495 Summer Street Room 627 Boston, MA 02210-2109				10. SPONSOR/MONITOR'S ACRONYM(S)	
				11. SPONSOR/MONITOR'S REPORT NUMBER(S) 1	
12. DISTRIBUTION/AVAILABILITY STATEMENT Approved for public Release distribution is Unlimited					
13. SUPPLEMENTARY NOTES					
14. ABSTRACT This report describes the technical progress towards the development of wide-band chaotic lidar technologies designed to provide performance improvements in turbid water					
15. SUBJECT TERMS Chaotic Lidar					
16. SECURITY CLASSIFICATION OF:			17. LIMITATION OF ABSTRACT	18. NUMBER OF PAGES	19a. NAME OF RESPONSIBLE PERSON
a. REPORT	b. ABSTRACT	c. THIS PAGE			19b. TELEPHONE NUMBER (Include area code)

20150309440

Award Information

Award Number	N000141010906
Title of Research	Chaotic LIDAR for Naval Applications
Principal Investigator	William D. Jemison
Organization	Clarkson University

Technical Section

Technical Objectives

The technical objectives of the project were identified in the original proposal as three tasks:

- Task 1 involves the generation and characterization of a wideband CLIDAR signal suitable for system-level experiments.
- Task 2 involves a system-level investigation into the underwater propagation/scattering characteristics of the CLIDAR signals. The investigation will be performed as a function of both optical wavelength and water turbidity (absorption and scattering) in order to determine the range resolution/accuracy and signal to noise performance that can be expected using CLIDAR.
- Task 3 involves the development of an advanced chaotic laser, or CLASER, for use as a compact and cost-effective optical source for CLIDAR. This approach integrates a laser gain medium into an OOR to produce an integrated chaotic optical source.

Technical Approach

The technical approach taken to develop the chaotic laser is shown in Figure 1. The chaotic laser (CLASER) signal source (block 1) is a 1064 nm infrared ytterbium-doped fiber laser (YDFL), which outputs a >1 GHz noise-like chaotic intensity modulation. This signal is amplified by a 2-stage fiber amplifier chain to boost the signal power to 6W. A free space frequency doubling crystal is then used to generate a blue-green wavelength. This 200mW signal is used with a digital receiver to form a chaotic LIDAR (CLIDAR) ranging system. The design of the chaotic fiber ring laser and the fiber amplifiers are guided by laser simulation tools developed under the project. Ranging experiments are performed in a small water tank to investigate CLIDAR system performance.

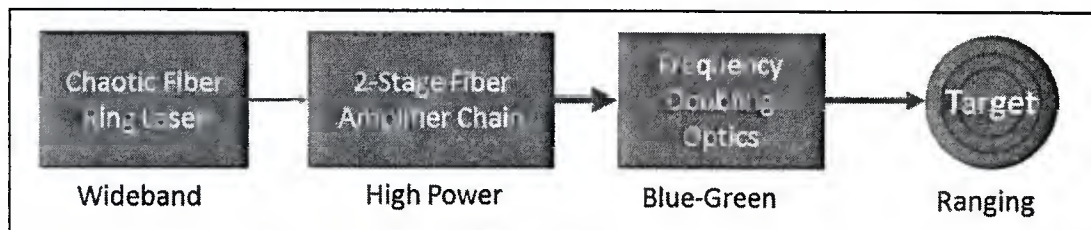


Fig 1. The chaotic LIDAR (CLIDAR) transmitter approach. Several stages are used to generate high power blue-green light suitable for underwater ranging. Experiments are performed in a small water tank.

Progress Statement Summary

A 532 nm chaotic laser (CLASER) transmitter was developed to investigate the performance of wideband chaotic lidar (CLIDAR) for naval underwater applications. The transmitter was built using a frequency doubled infrared fiber laser. Multiple fiber laser architectures were studied, built, and tested. A novel ultralong cavity (~100m) ring resonator was implemented for its noise-like chaotic intensity modulation. This laser generated wideband intensity modulation in the laser itself and did not require a separate optical modulator or RF signal source. The final configuration produced two hundred milliwatts of power at 532 nm with > 1GHz of noise-like chaotic intensity

modulation bandwidth. These power and bandwidth levels can support high resolution ranging and sensitive detection, and are attainable because of the fiber-based approach used. The transmitter design was aided by the development of an open-source custom fiber laser and fiber amplifier simulator. The simulator, implemented in MATLAB, included an analytical small signal gain calculation, an analytical laser performance calculation, and a custom numerical optical power simulator designed to efficiently handle the simulation of the long active fibers and high powers used in the CLIDAR fiber amplifiers. The performance of the simulator was validated against results in the literature and against experiments performed on the lasers developed under this project - the agreement between simulated results and experimental results was excellent.

CLIDAR system laboratory experiments were performed in clear and turbid water in a small water tank. Unambiguous ranging with sub-inch accuracy was demonstrated and target movements as small as $1/8^{\text{th}}$ inch were accurately detected using cross correlation signal processing. Both single and multiple targets were detected simultaneously with high accuracy. In turbid water, the location (*i.e.* range) of the volumetric backscatter return is also detected using the CLIDAR system. The ability to discriminate between the range and shape of the volumetric backscatter and the target returns should enable enhanced target detection in high turbidity by applying signal processing techniques used in other systems, although this was not investigated in this project. Experiments were performed to assess the effectiveness of the inherent wide bandwidth of the CLIDAR signal to suppress backscatter. Eliminating the low frequency content ($<100\text{MHz}$) from the received CLIDAR return via filtering significantly reduces the backscatter, as expected, with a minimal degradation of the target signal amplitude. While these results are promising, additional work is required to develop a calibration process for the CLIDAR system that will allow an accurate quantitative assessment of CLIDAR's backscatter reduction capability.

Progress

In the first fiscal year we reported the development of wideband noise-like chaotic signals using low-power fiber ring lasers operating at infrared wavelengths. Multiple infrared chaotic laser (CLASER) configurations were designed, built, and characterized in order to determine the best CLASER configuration to generate the desired signal, which was attained using a novel ultralong cavity approach. We also initiated the design and testing of a free space frequency doubler to convert the infrared signal to blue-green.

In the second fiscal year we fully designed and built all the necessary components for the blue-green chaotic CLIDAR source (infrared chaotic laser, fiber preamplifier, fiber gain amplifier, and frequency doubler) and integrated them into a working CLIDAR transmitter. This transmitter consists of a low-power chaotic infrared fiber laser source, two fiber amplifier stages, and a frequency doubler to convert the wavelength from 1064 nm to 532 nm. The completed CLIDAR transmitter operates at 150 mW continuous output power at 532 nm, with a noise-like chaotic signal of >1 GHz bandwidth. A detailed block diagram of the CLIDAR transmitter is shown in Figure 2, and a photograph of the assembled CLIDAR transmitter is shown in Figure 3. Custom computer code was developed to solve the rate equations governing rare-earth doped fiber lasers and amplifiers, and this code was used to design the laser and amplifiers for the CLIDAR transmitter. This simulation code has also been packaged and published as a design toolbox for use by the research community, and has been downloaded several hundred times to date.

Also in the second fiscal year, the CLIDAR transmitter was used with a photomultiplier tube (PMT) and a digital receiver to implement a CLIDAR ranging system. This system was used to perform unambiguous ranging in a water tank in clear water, where $< 1/2$ inch accuracy and ± 2 inch resolution were demonstrated.

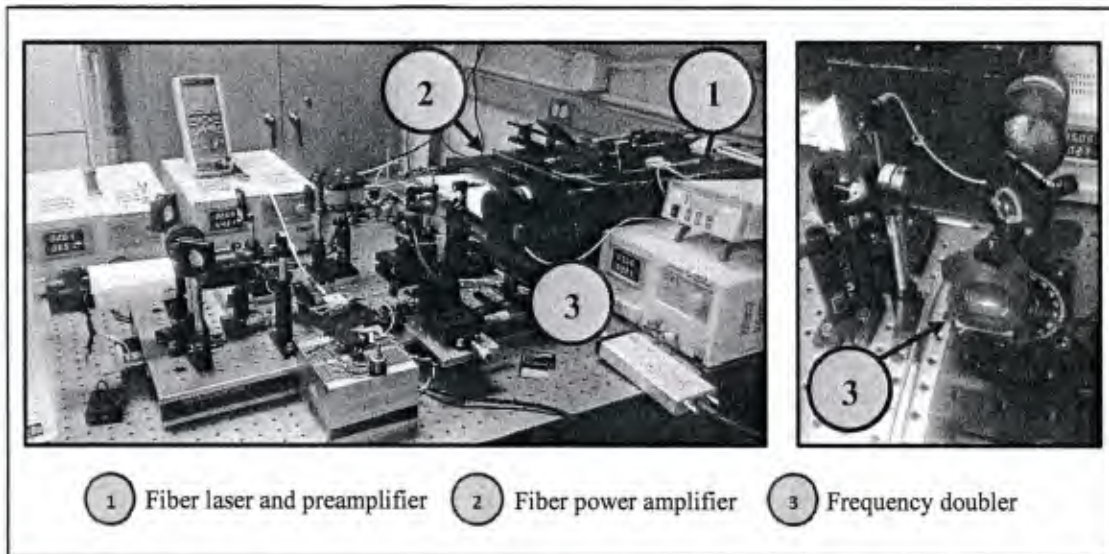


Fig 3. Photographs of the CLIDAR transmitter. Left: The fiber laser, fiber amplifiers, and frequency doubler generate the CLIDAR signal. Right: The frequency doubler generates green light from the infrared light.

In the current fiscal year, we made some minor improvements to the CLIDAR transmitter, increasing the output power to 200mW and increasing the laser bandwidth. We investigated additional system experiments in both clear and turbid water.

CLIDAR Transmitter Improvements – Several CLASER fiber splices were redone, and pump power levels were increased, resulting in an increase in CLIDAR transmitter output power from 150mW to 200mW, and an increase in the CLIDAR signal bandwidth. Figure 4 shows representative plots of the time domain, frequency domain, autocorrelation, and chaotic attractor plot of the CLIDAR transmitter. Figure 5 shows the simulated and experimental power curves for the CLIDAR's fiber amplifiers, which is an example of the excellent agreement obtained between computer simulations and experimental results.

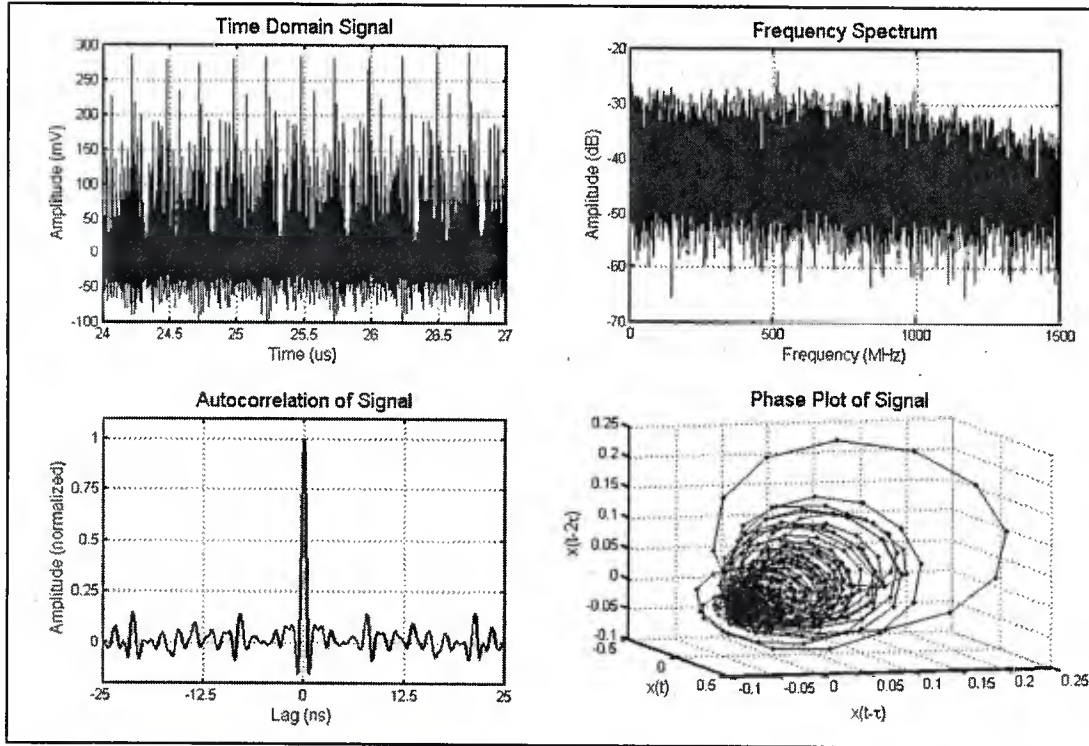


Fig 4. The CLIDAR transmitter intensity modulation signal. Top left: Time-domain view of the noise-like signal. Top right: The frequency-domain shows a wideband spectrum. Bottom left: The autocorrelation function is a sharp narrow peak. Bottom right: The phase plot shows an attractor shape typical of chaotic systems.

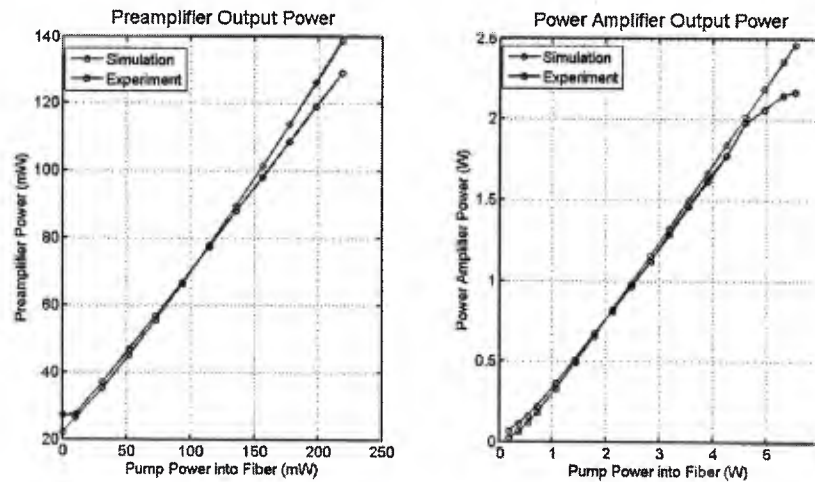


Fig 5. Power output of the CLIDAR transmitter. Left: Preamplifier simulation and experimental results. Right: Power amplifier simulation and experimental results up to 5 W output.

System Experiments - A block diagram of the system experimental set-up is shown in Figure 6. Targets in a small water tank can be precisely moved on a translation stage. The water turbidity can be varied via the use of liquid

antacid using a process reported by Dr. Mullen and her colleagues. Experimental turbidities reported here are measured with a WetLabs CSTAR turbidity meter.

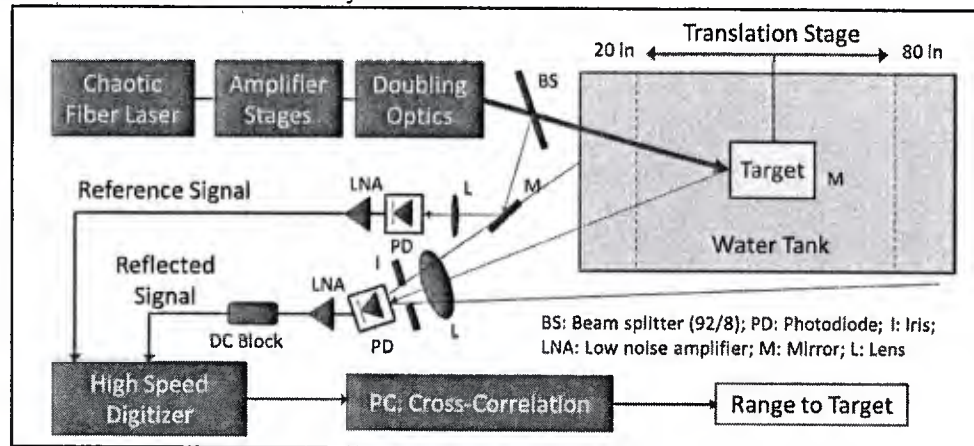


Fig 6. CLIDAR system experimental setup for underwater ranging tests.

Resolution Measurements - Figure 7 shows the results from a range resolution test. In this test, a black target was moved in increments as fine as $1/8^{\text{th}}$ inch. The test was conducted in clear water and is therefore representative of the best-case resolution performance given the existing photomultiplier tube (PMT) bandwidth and data collection system. It should be noted that the CLIDAR transmitter has more bandwidth than the PMT. Therefore, the range resolution is limited by the PMT/receiver.

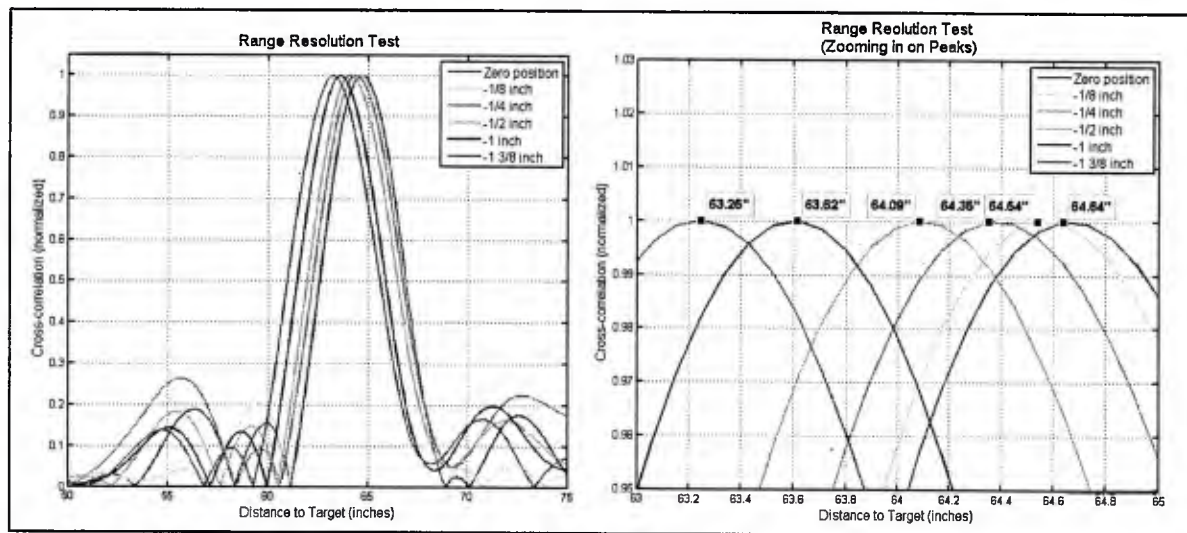


Fig 7. CLIDAR system experimental results: range resolution test using a black target, showing sub-inch range resolution.

Sensitivity Measurements – The sensitivity of the system was also investigated by varying the optical power transmitted to the target. Figure 8 shows the detection results for a fixed black target in clear water.

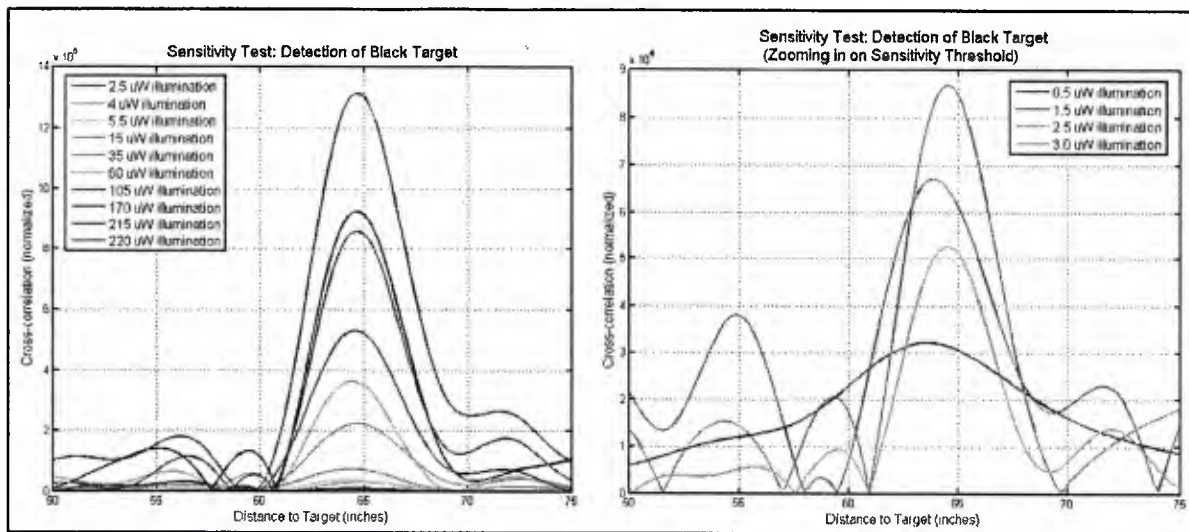


Fig 8. CLIDAR system experimental results: detection sensitivity, showing the potential of the system for detecting dark targets with low light levels.

Target Detection in Turbid Water – Figure 9 shows target detection at a variety of turbidities. The target, the volumetric backscatter response, and the response of a submerged mirror can all be seen in the range plots. While the backscatter response increases with increased turbidity, the target is detectable up to high turbidity with little change in measurement accuracy or peak width. In this test, gray and white targets were submerged, and the beam traveled through about 56” or 1.42m of turbid water on its way to the target. Thus the high turbidity case where the attenuation coefficient c is 3.5/m demonstrates the potential for sub-inch accuracy in about 5 attenuation lengths standoff distance.

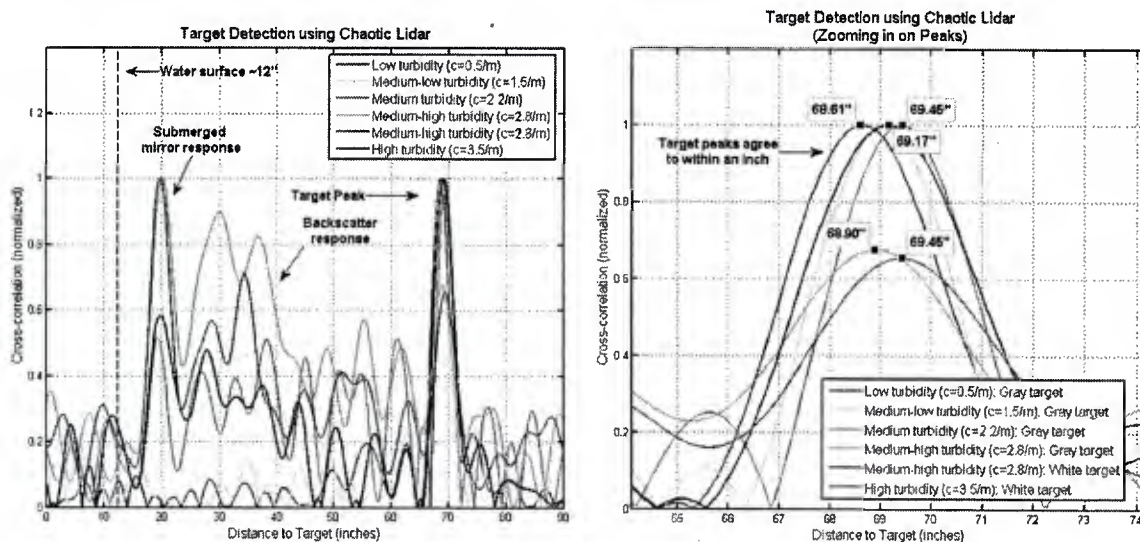


Fig 9. CLIDAR system experimental results: target ranging, demonstrating sub-inch detection accuracy at five attenuation lengths of turbid water.

Detection of Multiple Targets - Figure 10 shows the CLIDAR system's ability to detect multiple targets simultaneously. Two black targets were submerged at 13.25" separation in the tank. Data was taken for each target separately and then for both targets simultaneously.

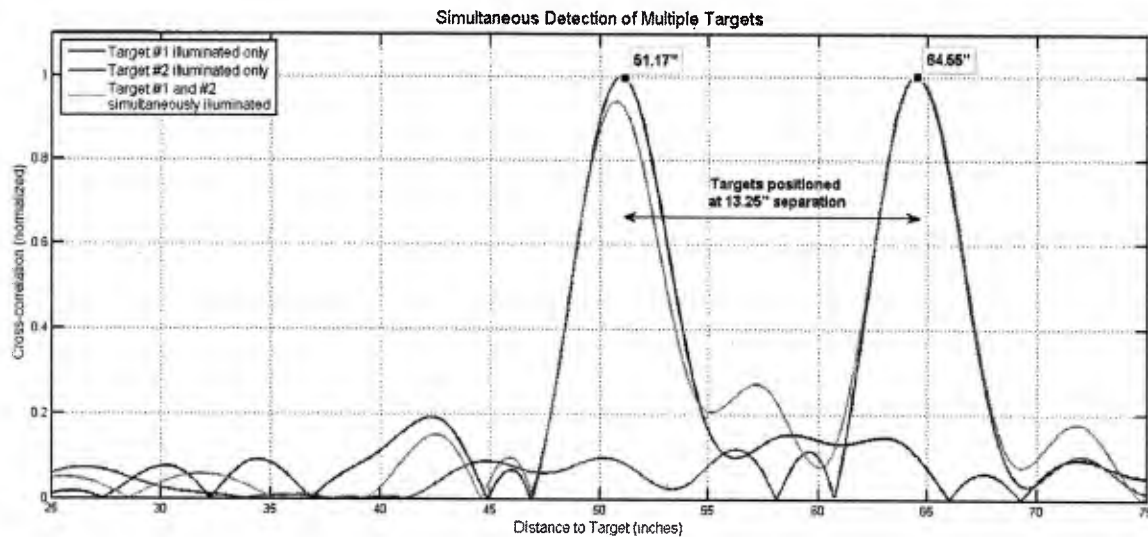


Fig 10. CLIDAR system experimental results: simultaneous multiple target detection. Two objects positioned 13.25 inches apart are illuminated by the beam and are detected by the CLIDAR system.

Backscatter Suppression – It is well known in hybrid lidar/radar that backscatter can be reduced by selecting a modulation frequency that is above ~100MHz. The CLIDAR waveform has instantaneous bandwidth that extends from low frequencies (~DC) into the GHz range. It is hypothesized that eliminating the CLIDAR frequencies below ~100MHz should provide backscatter suppression. Figure 11 shows the experimental results of a turbid water ($c=2.2, 2.8, 3.5$, i.e. harbor-like conditions) experiment where the full bandwidth of the CLIDAR signal was processed and the CLIDAR field of view was set to include both the range occupied by both the target and the volumetric backscatter. Both the target and the effects of volumetric backscatter can be seen.

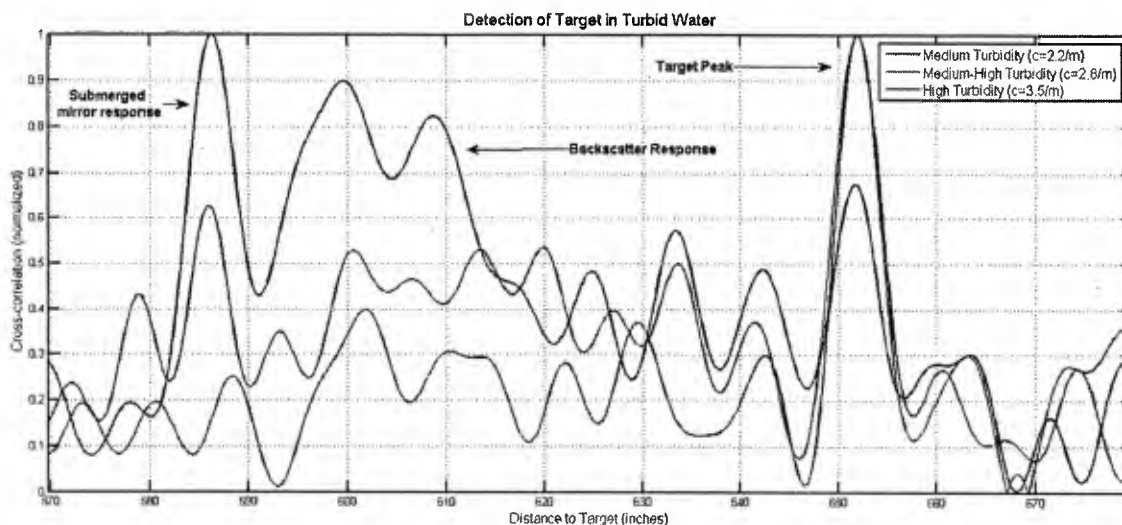


Fig 11. CLIDAR system experimental results: simultaneous backscatter and target detection. The broad response of the volumetric backscatter is seen on the left side of the graph, while the target peak is visible on the right.

Figure 12 shows the results for the same experiment when the low frequency content of the received signal is removed via filtering. A reduction on the backscatter response is clearly. The $c=3.5$ results also show the CLIDAR's ability to detect a target whose signal level is lower than the backscatter level. These results are very promising; however, additional work is required to calibrate the CLIDAR return in order to quantify the backscatter suppression.

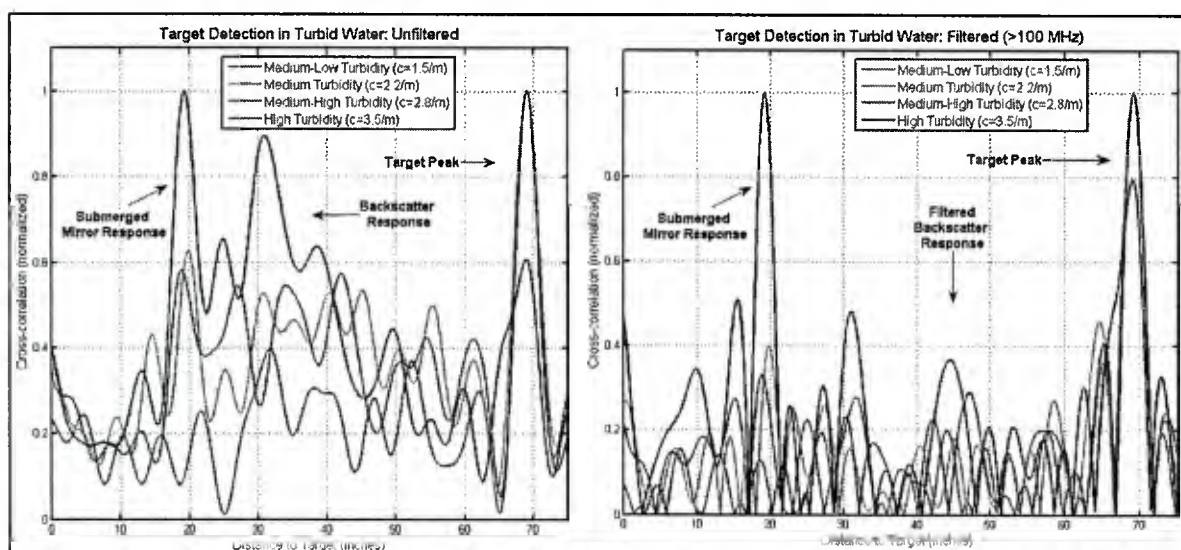


Fig 12. CLIDAR system experimental results: backscatter suppression and target detection. The volumetric backscatter response is attenuated by digital signal filtering, while the target peak remains strong and is slightly enhanced at $c=3.5/m$.